2011

Transverse Quantum Stern–Gerlach Magnets for Electrons

Scot McGregor
University of Nebraska - Lincoln

Roger Bach
University of Nebraska-Lincoln, roger.bach@gmail.com

Herman Batelaan
University of Nebraska - Lincoln, hbatelaan@unl.edu

New Journal of Physics
The open-access journal for physics

Transverse quantum Stern–Gerlach magnets for electrons

Scot McGregor, Roger Bach and Herman Batelaan[1]
Department of Physics and Astronomy, University of Nebraska—Lincoln, 208 Jorgensen Hall, Lincoln, NE 68588-0299, USA
E-mail: hbatelaan2@unlnotes.unl.edu

New Journal of Physics **13** (2011) 065018 (17pp)
Received 15 December 2010
Published 28 June 2011
Online at http://www.njp.org/
doi:10.1088/1367-2630/13/6/065018

Abstract. In the Stern–Gerlach experiment, silver atoms were separated according to their spin state (Gerlach and Stern 1922 *Z. Phys.* **9** 353–355). This experiment demonstrates the quantization of spin and relies on the classical description of motion. However, so far, no design has led to a functional Stern–Gerlach magnet for free electrons. Bohr and Pauli showed in the 1930 Solvay conference that Stern–Gerlach magnets for electrons cannot work, at least if the design is based on classical trajectories (Pauli W 1932 *Proc. of the 6th Solvay Conf. 2 (1930)* (Brussels: Gauthier-Villars) pp 183–86, 217–20, 275–80; Pauli W 1964 *Collected Scientific Papers* ed R Kronig and V F Weiskopf, vol 2 (New York: Wiley)). Here, we present ideas for the realization of a Stern–Gerlach magnet for electrons in which spin and motion are treated *fully quantum mechanically*. We show that a magnetic phase grating composed of a regular array of microscopic current loops can separate electron diffraction peaks according to their spin states. The experimental feasibility of a diffractive approach is compared to that of an interferometric approach. We show that an interferometric arrangement with magnetic phase control is the functional equivalent of an electron Stern–Gerlach magnet.

[1] Author to whom any correspondence should be addressed.

Contents

1. Introduction

Since Stern and Gerlach were able to separate the spin states of an unpolarized beam of silver atoms [1], one may ask, 'Can the same experiment be done with electrons?' In the 1930 Solvay Conference, Bohr and Pauli rejected four proposals regarding the separation of spin states for free electrons. Pauli's claim was that 'it is impossible to observe the spin of the electron, separated fully from its orbital momentum, by means of experiments based on the concept of classical particle trajectories' [2, 3]. An argument against the splitting of a free electron beam with a Stern–Gerlach magnet is that Lorentz forces will blur the effect of the spin-splitting forces.

The implications of the Bohr and Pauli statement have found their way into many contemporary textbooks [4–9] and have been interpreted to imply that the construction of an electron Stern–Gerlach magnet is impossible. In this paper, we do not address Bohr and Pauli's dictum but instead explore the possibility of an electron Stern–Gerlach magnet by considering *quantum trajectories*. That is, we take advantage of the quantum mechanical nature of the electron to force it into a motional quantum state in which spin splitting is possible. Such an idea has already been put forward for the longitudinal Stern–Gerlach magnet, for which the spin splitting is in the direction of motion [10]. For the longitudinal case, the motion is appropriately described by Landau states. These purely quantum mechanical motional states can be used to sidestep the issue of blurring due to the magnetic forces [10]. However, the question as to whether a quantum mechanical transverse Stern–Gerlach magnet exists for electrons has to our knowledge never been addressed. For the transverse case, the spin splitting is at normal angles to the direction of propagation of the electron, just as it is for the usual silver atom case. A transverse electron Stern–Gerlach magnet may provide an alternative technique for the production of polarized electron beams as compared with the usual optically pumped Ga-As sources [11]. The existence of a transverse Stern–Gerlach magnet (in addition to the earlier proposed longitudinal Stern–Gerlach magnet) addresses another proposal out of the four proposals rejected by Bohr and Pauli. This provides insights for finding a currently unknown dictum such as: 'It is possible to observe the spin of the electron, separated fully from its orbital momentum, by means of experiments based on the concept of *quantum* particle trajectories.'

In this paper, our main focus is on the fundamental question as to whether a transverse Stern–Gerlach magnet for electrons is possible in principle. To this end, we consider quantum

mechanical motion. The hallmark of quantum mechanical interference is that a final coherent state will be reached by at least two indistinguishable paths. The general idea is that along those paths, a different spin-dependent phase is applied to the electrons in each path. Upon recombination, a spin-dependent interference pattern will form. The techniques proposed for beam separation are diffraction with a magnetic phase grating (section 2) and interferometry with controlled Aharonov–Bohm and magnetic phases (section 3).

2. Stern–Gerlach diffraction

2.1. Magnetic phase grating

In Stern and Gerlach's original experiment, a beam of silver atoms was passed through a magnetic field gradient (figure 1(a)). The magnetic moments $\vec{\mu}$ of the atoms were directed transverse to the electron velocity $\vec{v}$ and (anti-)parallel to the magnetic field $\vec{B}$. The resulting classical motion of the atoms is governed by the interaction between the quantized spin and the magnetic field. The outcome is a beam that has been fully separated according to spin state.

For electrons, the original Stern–Gerlach arrangement would not work due to strong Lorentz forces. Brillouin proposed to use a longitudinal field (figure 1(b)) so that Lorentz forces could be neglected [12]. Pauli noted that although the spin states will be pushed apart by the inhomogeneous field of the Stern–Gerlach magnet, they will be blurred by a Lorentz force as a result of the gradient in the magnetic field orthogonal to the gradient, which is necessary for the splitting of the spins in the first place. The presence of the orthogonal field gradient is a consequence of Maxwell's equation that dictates that the divergence of the magnetic field is zero. Batelaan *et al* [13] found a mistake in Pauli's proof, but an analysis based on classical trajectories (with Landau state initial conditions) showed that the effect of Lorentz forces and spin forces were at best of the same strength, in keeping with the dictum of Bohr and Pauli. However, a fully quantum mechanical analysis [10] found that complete spin splitting is indeed possible due to quantization of orbital motion of Landau states. This scheme works when the width of the diffraction-limited electron beam is matched to the width of the lowest Landau state.

The new physical arrangement that we discuss in this section (figure 1(c)) is electrons passing through a grating where the applied magnetic field for each grating slit can be controlled separately. The quantization axis is chosen along the direction of motion. The electron velocity is parallel to the applied magnetic fields to avoid Lorentz forces, as in Brillouin's case. The motion must be treated quantum mechanically given that diffraction is a quantum phenomenon.

Currents in each loop are chosen in such a way that the magnetic field increases from one loop to the next in a stepwise manner across the grating (figure 1(c)). The magnetic field created by each loop induces a phase due to the $-\vec{\mu}\cdot\vec{B}$ interaction energy between the magnetic moment of the electron $\vec{\mu}$ and the applied field $\vec{B}$. This results in a phase shift for electrons that also increases in a stepwise manner. The phase shift difference for adjacent loops is chosen to be constant. The induced phase shifts for forward and backward spins are of opposite sign (figure 2).

Diffraction has the following general features. If the phase shift in each slit is spatially dependent and identical, then the envelope is determined by that spatial dependence, while the individual diffraction peaks' shape and position are unaffected. If the phase shift in each slit is spatially uniform but varies from slit to slit, the diffraction envelope is unaffected but the

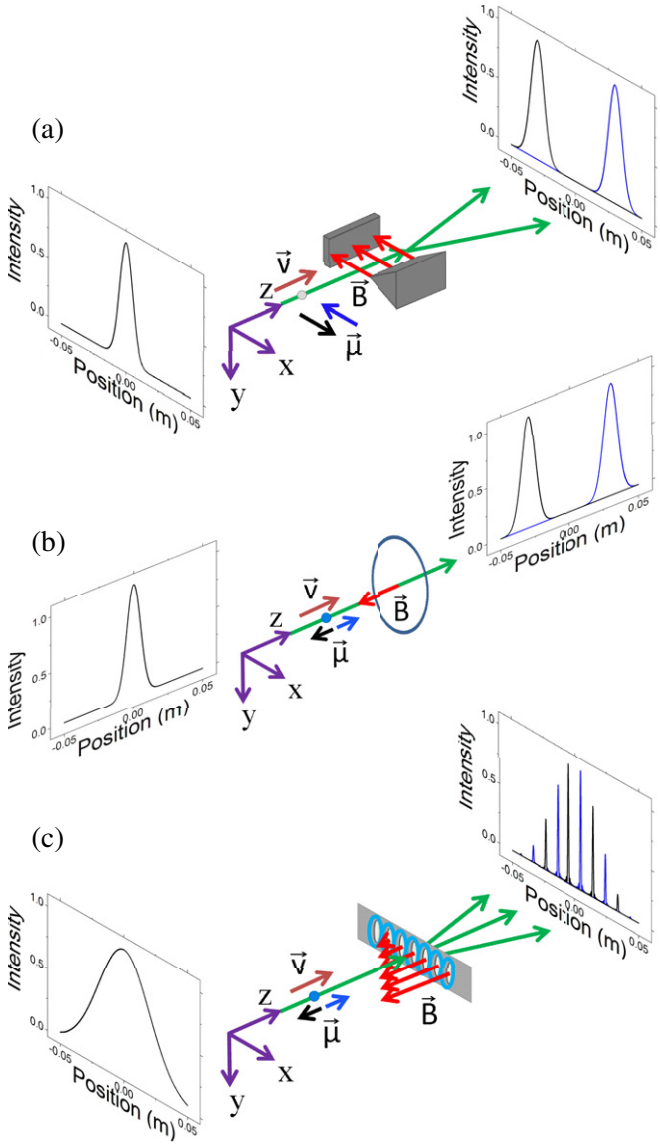

Figure 1. Stern–Gerlach systems. (a) In the original Stern–Gerlach experimental setup [1], a beam of silver atoms was split transverse to its direction of motion by an inhomogeneous magnetic field. (b) The longitudinal Stern–Gerlach magnet, originally conceived by Brillouin [12] and criticized by Pauli [2, 3], was reinstated by Batelaan and Gay [10, 13]. Electrons passing through a current-carrying loop obtain an additional spin-dependent phase due to the interaction energy of the magnetic moment of the electron and the magnetic field applied by the loop. Spin-forward/backward electrons are delayed/advanced in an arrangement that is a longitudinal Stern–Gerlach magnet (i.e. the splitting is along the direction of motion). (c) A quantum mechanical transverse Stern–Gerlach magnet for electrons is proposed in this paper. Current-carrying loops are placed in front of the slits of a grating in order to impart a phase on passing electrons, which depends on the spin of the electrons as well as on which slit they pass through. This causes the diffraction peaks for spin forward to be shifted oppositely to spin-backward peaks, transverse to the direction of motion.

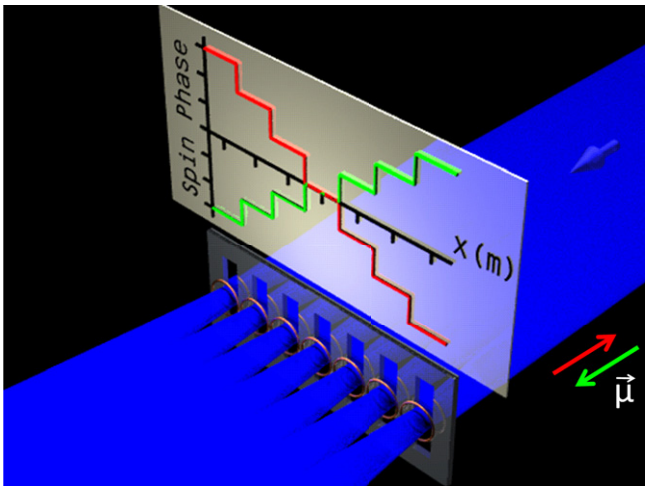

Figure 2. Magnetic phase grating. Electrons pass through current-carrying loops just after diffracting from the grating. The loops impart a phase that is spatially dependent in a stepwise manner. Each increment on the vertical axis is a $\pi/2$ phase shift and each mark on the horizontal axis indicates the location of a slit.

diffraction peaks shift, transverse to the direction of motion. The latter applies to the described physical system, which we refer to as a 'magnetic phase grating'.

According to Feynman's path integral formalism of quantum mechanics [14], the phase accumulated by an electron as it propagates along a path is given by the time integral of the Lagrangian [5] divided by Planck's constant,

$$\varphi = \frac{1}{\hbar}\int\left(\frac{p^2}{2m} + \vec{\mu}\cdot\vec{B} + q\vec{v}\cdot\vec{A}\right)\mathrm{d}t. \tag{1}$$

The phase shift due to p^2 (i.e. the first term in equation (1)) equals $2\pi L/\lambda_{\mathrm{dB}}$ in free space, where L is the length of the path and λ_{dB} is the de Broglie wavelength of the electrons. The phase due to the vector potential $\vec{A}$ (i.e. the third term in equation (1)) is discussed in detail in section 2.2.

The on-axis magnetic field for a loop of radius R [15] is

$$\vec{B} = B_0\frac{R^3}{(z^2+R^2)^{3/2}}\hat{z}, \tag{2}$$

where B_0 is the magnitude of the magnetic field at the center of the loop and $\hat{z}$ is directed along the axis. Performing the path integral over a straight trajectory along the $\hat{z}$-axis gives a phase shift

$$\begin{aligned}\varphi(x) &= \frac{1}{\hbar}\int_{-\infty}^{\infty}\vec{\mu}\cdot\vec{B}(x)\mathrm{d}t = \pm\frac{\mu B_0 R^3\sum_n H\left[x-(n-1/2)\,d\right]}{\hbar v_{\mathrm{e}}}\int_{-\infty}^{\infty}\frac{1}{(z^2+R^2)^{3/2}}\mathrm{d}z\\ &= \pm 2\frac{\mu B_0 R\sum_n H\left[x-(n-1/2)\,\mathrm{d}\right]}{\hbar v_{\mathrm{e}}},\end{aligned} \tag{3}$$

where v_{e} is the electron velocity, μ is the electron's magnetic moment, d is the grating's period, $n = 0, \pm1, \pm2, \ldots$ labels the slit and x is the coordinate parallel to the grating. The '$\pm$' sign in the second equality is because of considering spin up and down along the magnetic field

direction. The Heaviside function $H(x)$ is used to obtain an increasing stepwise function. The amplitude modulation imposed by the grating to an incident plane wave is

$$A(x) = \frac{1}{N}\sum_n \left\{ H\left[x - \left(nd + \frac{1}{2}w\right)\right] + H\left[x - \left(nd - \frac{1}{2}w\right)\right]\right\}, \tag{4}$$

where w is the slit width and N the total number of slits. The wave function after interaction with the grating is $\psi_{\text{grating}} = A(x)\mathrm{e}^{\mathrm{i}\varphi(x)}$, where φ and A are given by equations (3) and (4). Using the path integral formulation, the final quantum wave function at the detection plane is given by [16]

$$\psi_{\text{detect}}(x_{\text{d}}) = \int_{-\infty}^{\infty} K_{x_{\text{g}}\to x_{\text{d}}}(x_{\text{g}}, x_{\text{d}})\psi_{\text{grating}}(x_{\text{g}})\,\mathrm{d}x_{\text{g}}, \tag{5}$$

where x_{g} and x_{d} are the positions at the grating and the detector, respectively, ψ_{grating} is the wave function immediately after the grating, and $K_{x_{\text{g}}\to x_{\text{d}}}$ is the free space propagator,

$$K_{x_{\text{g}}\to x_{\text{d}}} = \exp\left[\frac{\mathrm{i}2\pi}{\lambda_{\text{dB}}}\sqrt{(x_{\text{d}} - x_{\text{g}})^2 + l^2}\right], \tag{6}$$

where λ_{dB} is the de Broglie wavelength and l is the distance from the grating to the detector. After the wave function is propagated, the probability distribution is $P(x_{\text{d}}) = |\psi_{\text{detect}}(x_{\text{d}})|^2$. Figures 3(a)–(c) show diffraction patterns corresponding to increasing magnetic field strengths. The velocity of the electrons is chosen to be $10^5\,\text{m}\,\text{s}^{-1}$, the period of the grating is 200 nm, the slit width is 15 nm, there are 25 slits each with a magnetic coil, and the distance from the grating to the detector is 53 cm. The parameters are motivated by experiments [17] except for the very low electron velocity. For now, Lorentz forces are ignored and the magnetic field is assumed to be uniform over the area of each slit, to simplify the exposition of the basic idea.

For zero currents, the electrons will simply diffract from the grating (figure 3(a)). When the current is increased, the two spin components each separate into a comb of diffraction peaks (figure 3(b)). For maximum spin separation, the necessary phase jump needed between adjacent slits is $\pi/2$ (figure 3(c)). The result is a spin-dependent displacement of the diffraction peaks within the diffraction envelope. The spin-forward electrons are displaced in an opposite direction as compared to the spin-backward electrons. The spin components are completely separated and motivate the nomenclature 'Quantum Stern–Gerlach Magnet'.

It is interesting to compare the above scenario to a *blazed* magnetic phase grating (for a regular blazed grating see [18]) to the above-discussed *stepped* magnetic phase grating. A blazed magnetic phase grating shifts the diffraction envelope in a spin-dependent manner while leaving the peak position unaffected. The affected envelope is representative of the single-slit diffraction pattern. Now the Bohr and Pauli argument applies directly; for a wide single slit where diffraction is small, the Lorentz force broadens the beam and overshadows the spin splitting. For a narrow single slit the Lorentz force can be reduced, but diffraction dominates the electron motion. Constructing a grating out of many such slits adds diffraction peaks, but, as mentioned above, these are not affected by spin. Thus, any such blazed grating Stern–Gerlach scheme is doomed to fail as either Lorentz forces or diffraction dominates the spin splitting effect, not allowing for full separation of the spin states.

2.2. *Lorentz blurring and spin flipping*

Given that Lorentz blurring is at the heart of the argument put forward by Bohr and Pauli, it is important that we include the Lorentz blurring in our calculation. In order to determine the

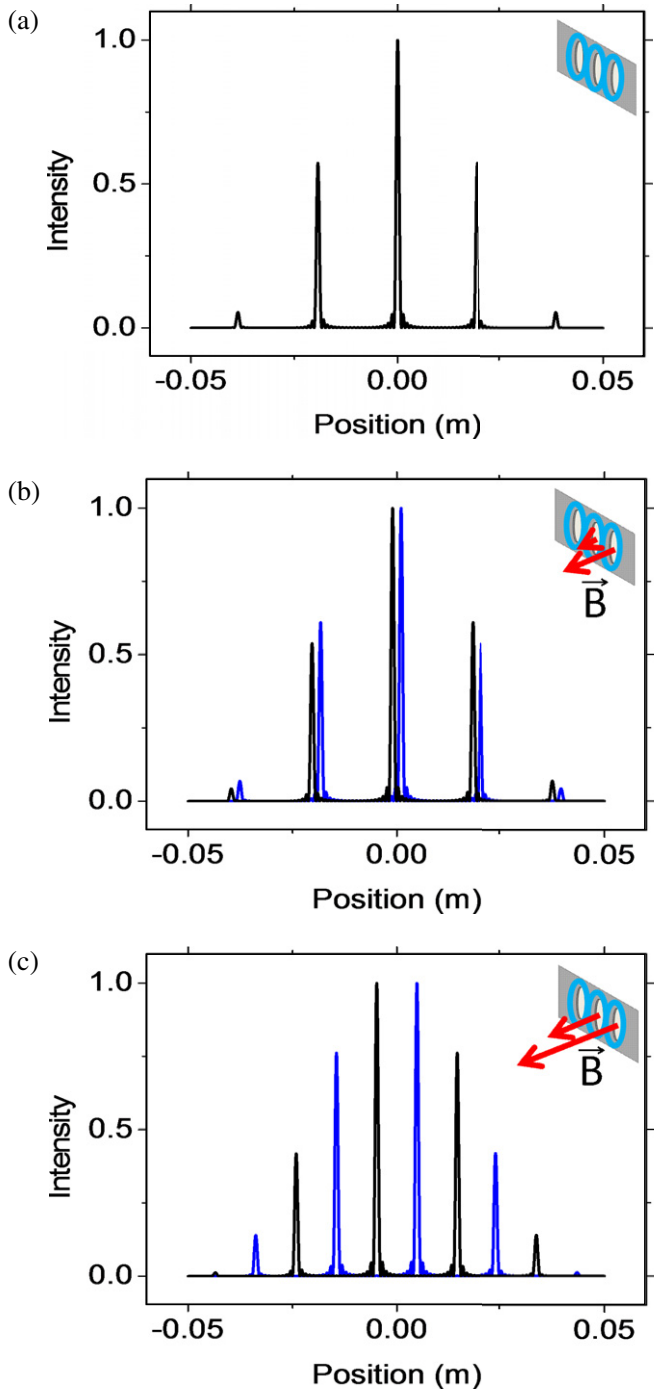

Figure 3. Spin-dependent electron diffraction patterns at varying magnetic field strengths without Lorentz blurring. (a) A familiar diffraction pattern is obtained when no magnetic field is applied. (b) A diffraction pattern with resolvable spin splitting is shown, when the magnetic field increment for adjacent slits is 1.8 T. (c) A diffraction pattern is shown when the magnetic field increment is 8.5 T, which shows maximum splitting. The phase shift between neighboring slits is $\pi/2$.

effects of the Lorentz force, the phase accumulated along a path is computed for an electron passing through the current-carrying loop (figure 4(a)). (Note that the path is not assumed to be straight but the classical trajectory obtained from solving the equation of motion, as appropriate for the path integral.) This phase can be used in the path integral calculation to determine the effect of Lorentz blurring on the interference pattern. The phase was calculated as a function of initial position for the electrons along the x-axis (figure 4(b)). The final value of the spin phase (due to the $-\vec{\mu}\cdot\vec{B}$ term) and Lorentz phase (due to the $q\vec{v}\cdot\vec{A}$ term) are calculated separately. The equations of motion [15] used for these trajectories is

$$\begin{aligned}
\frac{\mathrm{d}\vec{v}}{\mathrm{d}t} &= \frac{q}{\gamma m}\left[\vec{E}+\vec{v}\times\vec{B}-\frac{1}{c^2}\vec{v}(\vec{v}\cdot\vec{E})\right]+\nabla\left[\vec{\mu}\cdot\vec{B}+\frac{1}{c^2}(\vec{v}\times\vec{\mu})\cdot\vec{E}\right],\\
\frac{\mathrm{d}\vec{\mu}}{\mathrm{d}t} &= \frac{q}{m}\vec{\mu}\times\left[\left(\frac{g}{2}-1+\frac{1}{\gamma}\right)\vec{B}-\frac{1}{c^2}\left(\frac{g}{2}-1\right)\frac{\gamma}{\gamma+1}\vec{v}(\vec{v}\cdot\vec{B})-\frac{1}{c^2}\left(\frac{g}{2}-\frac{\gamma}{\gamma+1}\right)(\vec{v}\times\vec{E})\right],\\
\gamma &= \frac{1}{\sqrt{1-v^2/c^2}},
\end{aligned} \tag{7}$$

where $\vec{E}$ is electric field, g is the gyromagnetic ratio and c is the speed of light. For our purposes, $g=2$, $\gamma=1$ and $\vec{E}=0$, thus reducing the above equations to

$$\begin{aligned}
\frac{\mathrm{d}\vec{v}}{\mathrm{d}t} &= \frac{q}{m}\vec{v}\times\vec{B}+\frac{1}{m}\nabla(\vec{\mu}\cdot\vec{B}),\\
\frac{\mathrm{d}\vec{\mu}}{\mathrm{d}t} &= \frac{q}{m}\vec{\mu}\times\vec{B}.
\end{aligned} \tag{8}$$

The vector potential used is

$$\begin{aligned}
A_x &= \frac{-B_0R^3y}{2(R^2+x^2+y^2+z^2)^{3/2}},\\
A_y &= \frac{B_0R^3x}{2(R^2+x^2+y^2+z^2)^{3/2}},\\
A_z &= 0,
\end{aligned} \tag{9}$$

which is a valid approximation to second order in the position coordinates near the axis of the coil [15].

Figures 4(b) and (c) are calculated for a B_0 value of 8.5 T (to get a phase shift of $\pi/2$ for an interaction time of 0.8 ns). For the calculation in figure 3, the spin phase is assumed to be uniform across each individual slit. This assumption is not used for the results in figures 4(b) and (c). With initial conditions varying over a span of 15 nm, the spin-forward and -backward phase varies by less than 1%. It is apparent from figure 4(b) that the Lorentz phase will have a negligible influence on the spin splitting due to the fact that the difference in Lorentz phase accumulated by the two spin states is small compared to $\pi/2$. It does, however, have a parabolic shape. This is of little significance, however, as modulation of the shape of the phase in this way affects only the shape of the single-slit envelope but leaves the position and width of the much narrower diffraction peaks unaltered, thus in no way affecting the possibility of spin splitting (figure 4(c)).

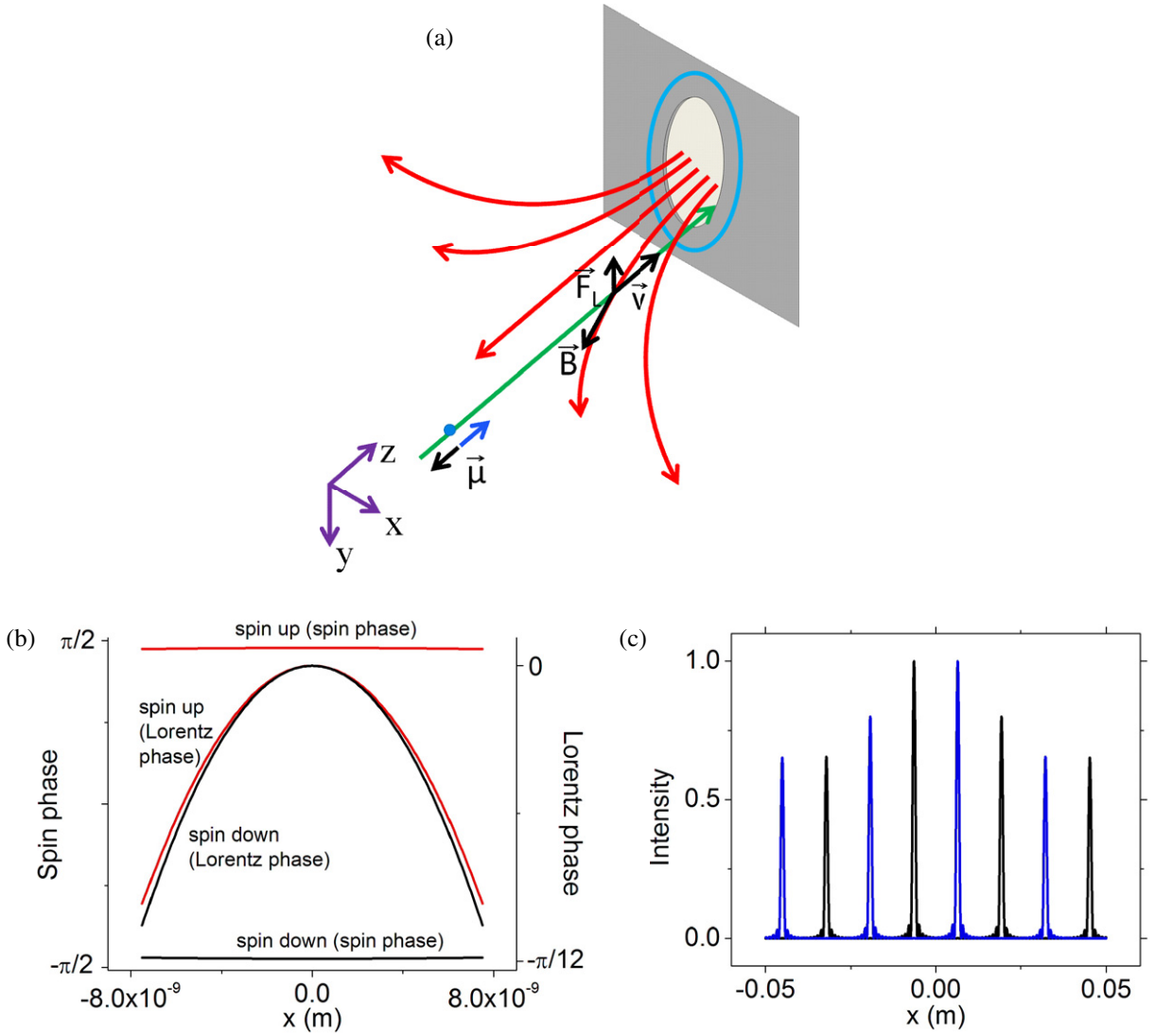

Figure 4. Lorentz blurring. (a) An electron entering a slit off-center experiences a Lorentz force and therefore accumulates a (Lorentz) phase accordingly. (b) The spin phase due to the magnetic interaction term $-\vec{\mu} \cdot \vec{B}$ is calculated along a path for electrons passing through a current-carrying loop as a function of initial position in x. It is approximately uniform. The Lorentz phase shift due to the interaction term $\vec{v} \cdot \vec{A}$, associated with the Lorentz force, is given for both spin states. The Lorentz phase shift difference between both spin states is much smaller than the spin phase difference for all x (note the separate scales on the vertical axes). (c) Spin splitting with the inclusion of Lorentz blurring, i.e. the spin-dependent parabolic phase shift at each slit due to the Lorentz phase, is taken into account in a fully quantum mechanical path integral calculation. The envelope of the diffraction pattern is modified, while the width and location of the individual diffraction peaks are not. Spin splitting remains in spite of the Lorentz force.

One so far unmentioned assumption is the absence of spin flipping. If the probability of spin flipping is large, then even when the diffraction peaks are maximally separated, the peaks are not spin polarized as many of the electrons will have spin flipped. To estimate the spin flip probability, the final orientation of the spin is calculated. Ehrenfest's theorem yields the time evolution of the quantum mechanical expectation value of the magnetic moment of an electron in a uniform magnetic field,

$$\frac{\mathrm{d}\langle\vec{\mu}\rangle}{\mathrm{d}t} = \frac{q}{m}\langle\vec{\mu}\rangle \times \vec{B}. \tag{10}$$

Therefore, the expectation value of the magnetic moment has the same time dependence as the solution to the classical equation of motion (equation (8)). The magnetic moment is calculated for a path passing through the current-carrying loop. The relative variation of the magnetic moment is very small. It can be shown by integration that the final value of the z-component only varies by about 0.08% over a range of initial positions of 15 nm, thus illustrating the negligible probability of spin flipping, and justifying the use of equation (10).

Another effect that in principle contributes to the phase shift is image charge interaction [16, 17]. Image charge can affect the electron trajectory as well as time evolution of the magnetic moment (see equation (7)). Effects on the electron trajectory are the same for each slit and as such affect only the envelope, therefore not affecting the spin splitting in any way. Also, any spin evolution terms that depend on the electric field are proportional to $1/c^2$ and are therefore very small compared with the spin evolution in the magnetic field.

While the above arguments demonstrate that the transverse spin splitting of a free electron beam is, in principle, possible, it is, by the means described in this paper, not experimentally feasible due to the large magnetic fields and low-energy electrons. These problems can possibly be addressed in a number of ways. The demand for high magnetic fields can be reduced by applying the spin-dependent phase modulo 2π. In the configuration described above, the spin-dependent phase follows the pattern 0, $\pi/2$, π, $3\pi/2$, 2π, $5\pi/2$ and so on. If we take those values modulo 2π the pattern would simply repeat the values 0, $\pi/2$, π and $3\pi/2$ allowing for lower magnetic fields in many of the coils. Secondly, we can increase the length of the region in which the electron has appreciable interaction with the magnetic field. This can be done by replacing the loop by a solenoid. Doing so would allow for a combination of lower magnetic fields and higher electron energy. The small separation of the slits makes this, even with modern nano-fabrication technology, a very challenging proposition.

3. Stern–Gerlach interference

3.1. The magnetic phase interferometer

Consider the interferometer shown in figure 5. In such an interferometer, an electron beam is split into two beams. Each beam passes through a solenoid. After the beams pass through the solenoids, they are recombined and interference fringes are observed.

The solenoids are set up to create magnetic fields of equal magnitude but opposite direction, which are parallel to the direction of motion of the electrons to reduce Lorentz forces. When the magnetic field is turned on, the fringes corresponding to spin-forward electrons will shift one way and the fringes corresponding to spin-backward electrons will shift the other way. Here we

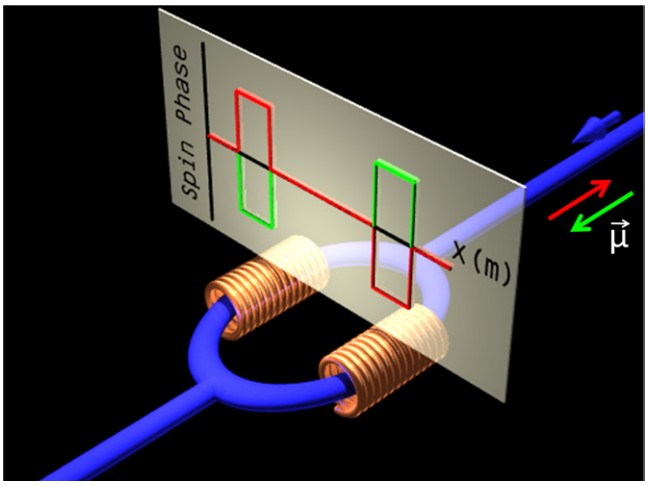

Figure 5. Magnetic phase interferometer. An electron interferometer with a solenoid around each arm creates a spin-dependent phase difference between the two arms. The graph indicates the phase accumulated by the electrons as they pass through the solenoids. The green and red curves represent spin up and down, respectively. It is proposed that this arrangement will control the electron polarization of the output, as explained below.

consider a solenoid 1 cm long with a radius of 1 mm. A 1 micron diameter beam of electrons enters the solenoid at $5 \times 10^6\,\mathrm{m\,s^{-1}}$. Here we used the following vector potential,

$$A_x = \frac{\mu_0 K R^2 y}{4\left(R^2+x^2+y^2\right)}\left(\frac{z-L/2}{\sqrt{R^2+x^2+y^2+(z-L/2)^2}} - \frac{z+L/2}{\sqrt{R^2+x^2+y^2+(z+L/2)^2}}\right),$$
$$A_y = \frac{\mu_0 K R^2 x}{4\left(R^2+x^2+y^2\right)}\left(\frac{z+L/2}{\sqrt{R^2+x^2+y^2+(z+L/2)^2}} - \frac{z-L/2}{\sqrt{R^2+x^2+y^2+(z-L/2)^2}}\right), \quad (11)$$
$$A_z = 0.$$

The vector potential for a solenoid with length L was constructed by integrating the vector potential in the continuous limit of a series of loops (equation (9)) [15]. In these equations, μ_0 is the permeability of free space, K is the surface current density in the solenoid, and R is the radius of the solenoid. The spin-dependent phase was integrated along the classical curved path (figure 6(a)) and found to be uniform across the solenoid (figure 6(b)).

The Lorentz phase was, as before, quadratic in initial position but not dependent on spin (figure 6(b)). These calculations were made for a solenoid with a modest surface current density equal to $7100\,\mathrm{A\,m^{-1}}$, which gives the spin-forward electrons passing through the solenoid a phase shift of $\pi/2$. The probability of spin flipping is low ($< 3 \times 10^{-7}$) in this case as it is in the example of the magnetic phase grating.

3.2. The grating bi-prism interferometer

Consider a wide angle beam splitter consisting of a grating and a bi-prism wire, such as the one described by Caprez *et al* [19]. Figure 7 depicts a setup using this beam splitter to separate (albeit not fully) spin states interferometrically.

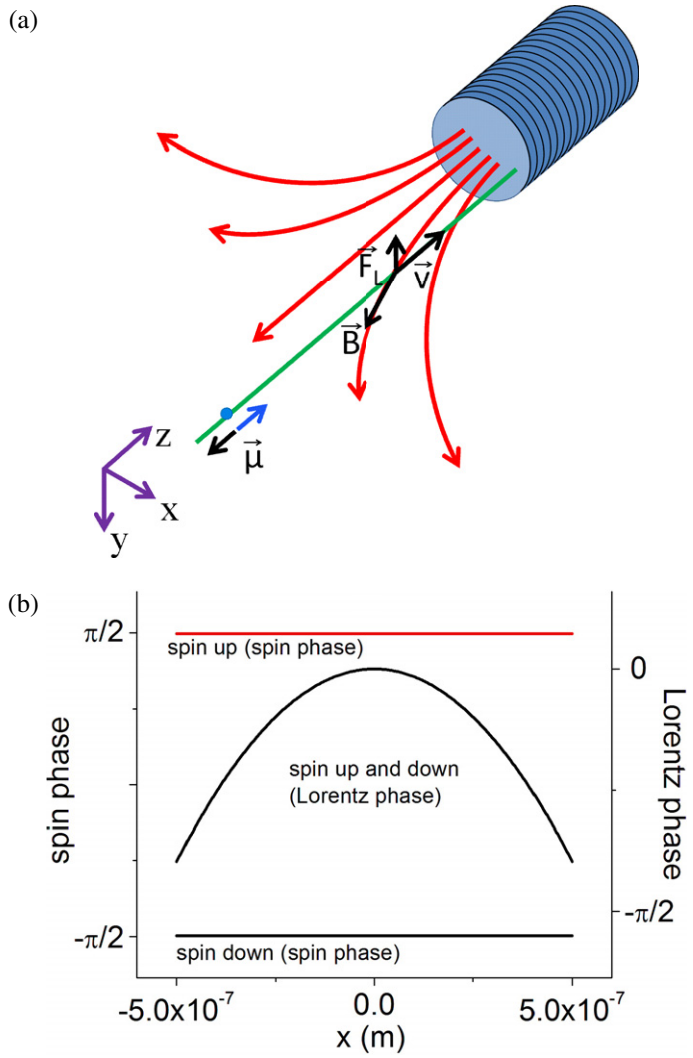

Figure 6. Lorentz blurring for a solenoid. (a) An electron entering the solenoid off-center experiences a Lorentz force and therefore accumulates a (Lorentz) phase accordingly. (b) The spin phase term is uniform across the solenoid in the region of interest, as in the previous case involving the phase grating. The Lorentz phase term is quadratic and spin independent, as in the previous case involving the phase grating.

The interferometer shown above consists of a grating, two bi-prisms, two solenoids, an electrostatic quadrupole lens and a spatial detector. The zero diffraction order is blocked by the first bi-prism wire. A negative voltage is applied to the first bi-prism to push the two first diffraction orders away from each other. This is necessary to create space for the solenoids. A positive voltage is applied to the second bi-prism to bring the two beams back together. The two beams pass through solenoids as they approach a quadrupole lens that magnifies the interference pattern. By applying a current to the solenoids, a spin-dependent phase difference is created between the two arms of the interferometer. This would result in opposite fringe shifts for spin up as compared with spin down electrons.

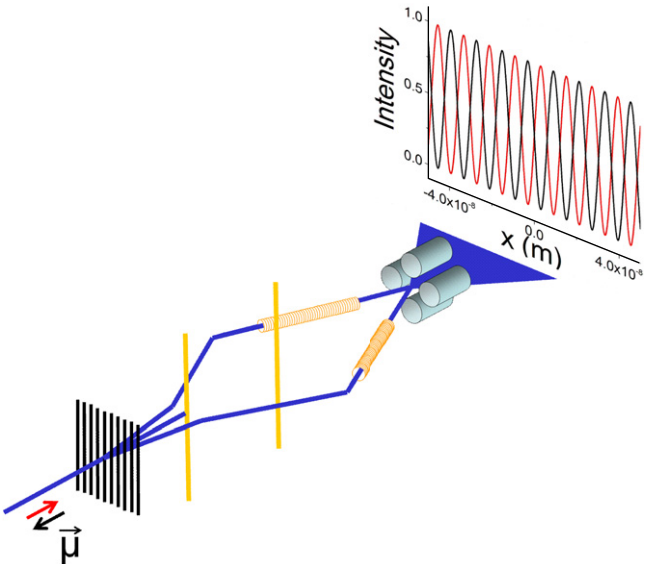

Figure 7. Grating bi-prism interferometer. An electron beam passes through a grating. The zero-order and the two first-order diffracted beams are shown. The first bi-prism wire blocks the zero order while pushing the two first-order beams away from each other. The second bi-prism brings the two first-order beams back together. They pass through solenoids on their way to the quadrupole lens where the image of the fringes is magnified and projected onto the detection plane. Near-field interference patterns for spin-up and spin-down states (red and black) are shifted with respect to each other.

Figure 8(a) depicts the interference fringes with no current being applied to the solenoids. Figure 8(b) shows a similar fringe pattern but this time with a surface current density of $3550\,\mathrm{A\,m^{-1}}$, the current required for a $\pi/4$ magnitude phase shift in each arm. This result is obtained from a full path integral simulation including a bi-prism and two beams propagating through finite length solenoids (including Lorentz blurring). This scenario is more feasible (than the example of the phase grating) as a large separation between the arms of the interferometer allows for larger coils to be inserted.

3.3. The Mach–Zehnder interferometer

To achieve full spin splitting, consider a Mach–Zehnder interferometer that consists of two sets of unfocused counter-propagating laser beams and three bi-prism wires (figure 9) [20] in a similar configuration to the previous example.

The electrons Bragg scatter from the laser beams as described by Freimund *et al* [21]. Two balanced electron beams emerge from a perfect Bragg crystal. In between the two arms of the interferometer, a solenoid is placed perpendicular to the electron beams, which provides an Aharanov–Bohm phase shift [22]. The purpose of this phase shift is to balance the electron intensity of the two interferometer output beams. A solenoid in each interferometer arm provides a spin-dependent phase shift causing electron polarization of the two outputs. As with the grating bi-prism interferometer example (section 3.2), the large separation allows for long interaction times, thus minimizing the necessary magnetic field as well as allowing for

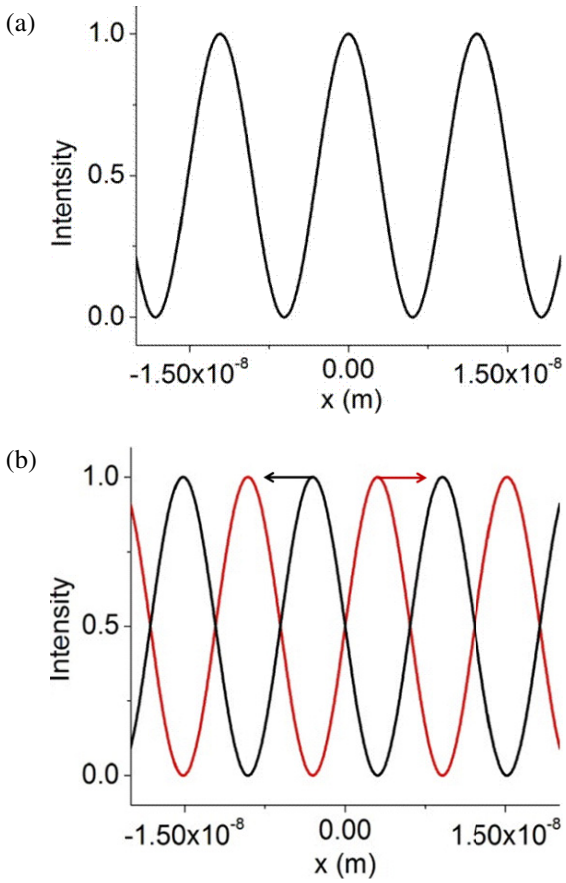

Figure 8. Near-field fringes. (a) Interference fringes are calculated with no current in the solenoids. (b) Interference fringes are calculated with each solenoid carrying a surface current density of 3550 A m^{-1}. The arrows show the direction in which the fringes shift for each spin state as the current is increased.

higher-energy electrons. For this configuration, a path integral computation yields the probability for spin-forward and spin-backward detections as a function of the current in the two solenoids, taking into account Lorentz blurring (figure 9). Complete separation of the two spin states in two beams is obtained (figure 9, inset) as one would hope to get for a perfect electron Stern–Gerlach magnet.

A quantum optical analysis of this system based on two momentum states and two spin states yields the same result. Consider an unpolarized input state with a downward component of momentum (figure 10) described by the density operator

$$\rho_{\text{initial}} = \tfrac{1}{2}\left(|+\rangle_-\langle +|_- + |-\rangle_-\langle -|_-\right), \tag{12}$$

where a '+' or '−' inside the bras and kets indicates spin forward or backward, while a '+' or '−' subscript indicates an upward or downward component of momentum (as related to figure 10).

The effect of the beamsplitter described by

$$\begin{aligned} |+\rangle_- &\xrightarrow{\text{BS}} \frac{\sqrt{2}}{2}\left(i|+\rangle_+ + |+\rangle_-\right), \\ |+\rangle_+ &\xrightarrow{\text{BS}} \frac{\sqrt{2}}{2}\left(i|+\rangle_- + |+\rangle_+\right) \end{aligned} \tag{13}$$

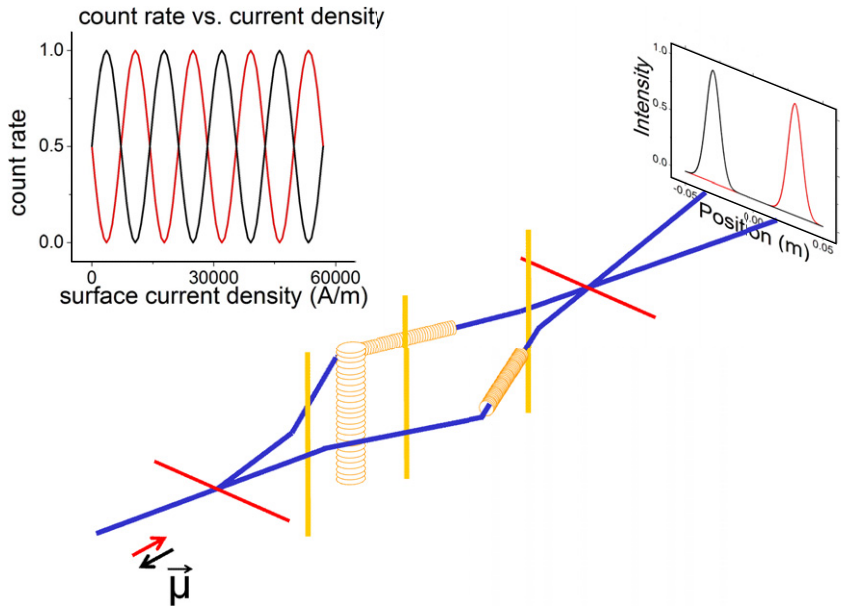

Figure 9. Mach–Zehnder interferometer. The interferometer consists of two sets of counter-propagating laser beams (horizontal red lines) and three bi-prism wires. A solenoid enclosed by the two interferometer arms creates an Aharanov–Bohm phase shift to balance the interferometer (see text). Solenoids are placed around each arm to create a spin-dependent phase shift, which polarizes the two outputs of the interferometer. The graph shown is the result of a path integral calculation of the count rate in one of the arms as a function of current density in the solenoids. The two curves are the count rates of the two spin states.

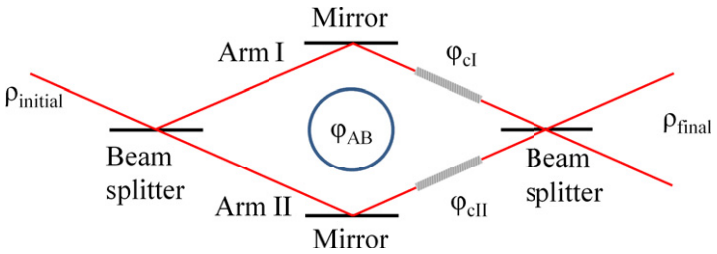

Figure 10. Schematic diagram of the interferometer. The operational elements of the Mach–Zehnder interferometer are indicated (for a detailed description, see text).

is independent of spin. The effect of the mirror described by

$$|+\rangle_- \xrightarrow{\mathrm{M}} i|+\rangle_+, \qquad |+\rangle_+ \xrightarrow{\mathrm{M}} i|+\rangle_- \tag{14}$$

is also independent of spin. The AB phase shift and the phase shift given by the coils are dependent on which arm of the interferometer the electrons go through. The arms are labeled I and II to track these phase shifts. The phase shifts given by the coils are chosen to be of equal

magnitude and opposite sign. In arm I, the phase shift given by the coil and the AB phase shift are given by

$$\begin{aligned}
&|+\rangle_- \xrightarrow{\text{Coil}} \exp(\mathrm{i}\varphi_c)\,|+\rangle_-,\\
&|-\rangle_- \xrightarrow{\text{Coil}} \exp(-\mathrm{i}\varphi_c)\,|-\rangle_-,\\
&|+\rangle_- \xrightarrow{\text{AB}} \exp\left(\frac{\mathrm{i}\varphi_{AB}}{2}\right)|+\rangle_-,
\end{aligned} \tag{15}$$

and in arm II these phase shifts are given by

$$\begin{aligned}
&|+\rangle_+ \xrightarrow{\text{Coil}} \exp(-\mathrm{i}\varphi_c)\,|+\rangle_+,\\
&|-\rangle_+ \xrightarrow{\text{Coil}} \exp(\mathrm{i}\varphi_c)\,|-\rangle_+,\\
&|+\rangle_+ \xrightarrow{\text{AB}} \exp\left(\frac{-\mathrm{i}\varphi_{AB}}{2}\right)|+\rangle_+,
\end{aligned} \tag{16}$$

where the AB phase shift is spin independent. The resulting output density operator is

$$\begin{aligned}
\rho_{\text{final}} = \tfrac{1}{8}\,&\{\exp[-\mathrm{i}\,(\varphi_c+\varphi_{AB}/2)]\,(|+\rangle_+ + \mathrm{i}|+\rangle_-) + \mathrm{i}\exp[\mathrm{i}\,(\varphi_c+\varphi_{AB}/2)]\,(|+\rangle_- + \mathrm{i}|+\rangle_+)\}\\
&\times\left\{\exp[\mathrm{i}\,(\varphi_c+\varphi_{AB}/2)]\,(\langle+|_+ - \mathrm{i}\,\langle+|_-) - \mathrm{i}\exp[-\mathrm{i}\,(\varphi_c+\varphi_{AB}/2)]\,(\langle+|_- - \mathrm{i}\,\langle+|_+)\right\}\\
&+\tfrac{1}{8}\,\{\exp[\mathrm{i}\,(\varphi_c-\varphi_{AB}/2)]\,(|-\rangle_+ + \mathrm{i}|-\rangle_-) + \mathrm{i}\exp[-\mathrm{i}\,(\varphi_c-\varphi_{AB}/2)]\,(|-\rangle_- + \mathrm{i}|-\rangle_+)\}\\
&\times\left\{\exp[-\mathrm{i}\,(\varphi_c-\varphi_{AB}/2)]\,(\langle-|_+ - \mathrm{i}\,\langle-|_-) - \mathrm{i}\exp[\mathrm{i}\,(\varphi_c-\varphi_{AB}/2)]\,(\langle-|_- - \mathrm{i}\,\langle-|_+)\right\}.
\end{aligned} \tag{17}$$

The probability of finding each spin state in each output is

$$\begin{aligned}
P_{++} &= \langle+|_+\,\rho_{\text{final}}|+\rangle_+ = \tfrac{1}{2}\sin^2(\varphi_c+\varphi_{AB}/2),\\
P_{-+} &= \langle-|_+\,\rho_{\text{final}}|-\rangle_+ = \tfrac{1}{2}\sin^2(\varphi_c-\varphi_{AB}/2),\\
P_{+-} &= \langle+|_-\,\rho_{\text{final}}|+\rangle_- = \tfrac{1}{2}\cos^2(\varphi_c+\varphi_{AB}/2),\\
P_{--} &= \langle-|_-\,\rho_{\text{final}}|-\rangle_- = \tfrac{1}{2}\cos^2(\varphi_c-\varphi_{AB}/2).
\end{aligned} \tag{18}$$

A non-zero AB phase shift ($\varphi_{AB} = \pi/2$) together with a non-zero spin-dependent phase shift ($\varphi_c = \pi/4$) is required to obtain complete spin splitting; $P_{++} = P_{--} = \frac{1}{2}$, $P_{+-} = P_{-+} = 0$.

4. Conclusion

The following question is addressed: 'Is it possible to observe the spin of the electron, separated fully from its orbital momentum, by means of experiments based on the concept of *quantum* particle trajectories?' As this applies to Stern–Gerlach 'magnets', the answer is affirmative. For the longitudinal case, this has been analyzed previously [10], while in this paper a transverse case is analyzed. The arrangement is not optimized for practical applications; magnetic Bragg crystals would be interesting to study in this context. Nevertheless, the logical argument is made for a scenario where the physical elements have been individually realized. The answer to the above question appears to be 'Yes'. For example, spin can be observed, fully separated from its orbital momentum, by energy jumps associated with spin flips, in the lowest quantum motional states (cyclotron and magnetron) [23]. Dehmelt has observed such spin

flips [23] for individual electrons, and attacked Bohr and Pauli's dictum [24], suggesting the above formulated general rule.

Acknowledgments

This work was supported by the National Science Foundation under grant no. 0969506 and by DOE-GAANN grant no. P200A0603110.

References

[1] Gerlach W and Stern O 1922 Das magnetische moment des silberatoms *Z. Phys.* **9** 353–5
[2] Pauli W 1932 *Proc. of the 6th Solvay Conf. 2 (1930)* (Brussels: Gauthier-Villars) pp 183–6, 217–20, 275–80
[3] Pauli W 1964 *Collected Scientific Papers* vol 2 ed R Kronig and V F Weiskopf (New York: Wiley) pp 544–52
[4] Baym G 1969 *Lectures on Quantum Mechanics* (New York: Benjamin)
[5] Cohen-Tannoudji C, Diu B and Laloë F 1977 *Quantum Mechanics* (New York: Wiley-Interscience)
[6] Merzbacher E 1970 *Quantum Mechanics* (New York: Wiley) p 254
[7] Mott N F and Massey H S W 1965 *The Theory of Atomic Collisions* (Oxford: Clarendon)
[8] Ohanian H C 1990 *Principles of Quantum Mechanics* (Englewood Cliffs, NJ: Prentice-Hall) p 1
[9] Wheeler J A 1983 *Quantum Theory and Measurement* ed W H Zurek (Princeton, NJ: Princeton University Press) p 699
[10] Gallup G A, Batelaan H and Gay T J 2001 Quantum mechanical analysis of a longitudinal Stern–Gerlach effect *Phys. Rev. Lett.* **86** 4508–11
[11] Rosenberry M A, Batelaan H, Reyes J P and Gay T J 2002 Correlations, polarization, and ionization *AIP Conf. Proc.* **604** 264–9
[12] Brillouin L 1928 Is it possible to test by a direct experiment the hypothesis of the spinning electron? *Proc. Natl Acad. Sci. USA* **14** 755
[13] Batelaan H, Gay T J and Schwendiman J J 1997 Stern–Gerlach effect for electron beams *Phys. Rev. Lett.* **79** 4517–21
[14] Feynman R P 1948 Space-time approach to non-relativistic quantum mechanics *Rev. Mod. Phys.* **20** 367–87
[15] Jackson J D 1999 *Classical Electrodynamics* (New York: Wiley)
[16] Barwick B, Gronniger G, Yuan L, Liou S and Batelaan H 2006 A measurement of electron-wall interactions using transmission diffraction from nano-fabricated gratings *J. Appl. Phys.* **100** 074322
[17] Gronniger G, Barwick B, Batelaan H, Savas T, Pritchard D and Cronin A 2005 Electron diffraction from free-standing, metal-coated transmission gratings *Appl. Phys. Lett.* **87** 124104
[18] Gao H, Gronniger G, Freimund D, Cronin A and Batelaan H 2002 Phase and absorption gratings for electrons *Int. Conf. on Atomic Physics XVIII* ed H R Sadeghpour, D E Pritchard and E J Heller (Singapore: World Scientific) pp 133–41
[19] Caprez A, Bach R, McGregor S and Batelaan H 2009 A wide-angle electron grating bi-prism beam splitter *J. Phys.* B **42** 165503
[20] Hasselbach F and Nicklaus M 1993 Sagnac experiment with electrons: observation of the rotational phase shift of electron waves in vacuum *Phys. Rev.* A **48** 143–51
[21] Freimund D L and Batelaan H 2002 Bragg scattering of free electrons using the Kapitza–Dirac effect *Phys. Rev. Lett.* **89** 283602
[22] Aharonov Y and Bohm D 1959 Significance of electromagnetic potentials in the quantum theory *Phys. Rev.* **115** 485–91
[23] Dehmelt H 1990 Experiments with an isolated subatomic particle at rest *Rev. Mod. Phys.* **62** 525–31
[24] Dehmelt H 1988 New continuous Stern–Gerlach effect and a hint of 'the' elementary particle *Z. Phys.* D **10** 127–34